Lucas, et al

SUPPLEMENTARY FIGURE S1

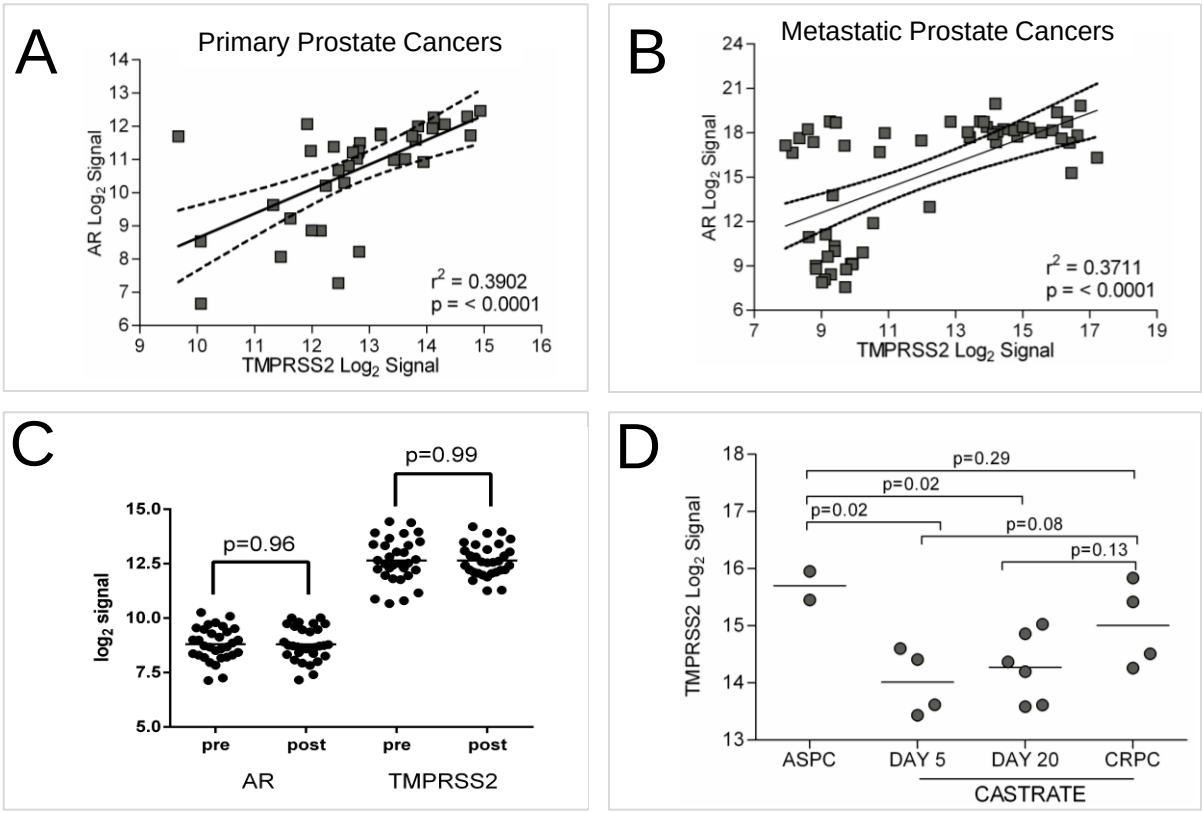

Supplementary Figure S1. TMPRSS2 expression is associated with androgen receptor (AR) levels and is regulated by androgens *in vivo*.

(A) Correlation TMPRSS2 and AR transcript levels determined from the same localized or
(B) metastatic tumor sample.
(C) To evaluate the effect of chemotherapy on the expression of TMPRSS2, we microdissected neoplastic prostate epithelium before (frozen prostate needle biopsies) and after (frozen radical prostatectomy tissue) exposure to 4 cycles of mitoxantrone and docetaxel chemotherapy. A total of 31 subjects were evaluated. Viable tumor cells were present for all subjects before (pre) and after (post) chemotherapy. To allow for accurate comparisons, approximately 2,000 neoplastic tumor cells were dissected from each pre-treatment and post-treatment sample. qRT-PCR was used to quantitate transcripts for TMPRSS2 and AR. There was no difference in the abundance of mRNAs encoding AR or TMPRSS2 pre/post treatment, either by overall groups, or comparing each patient pair.
(D) TMPRSS2 expression in androgen-sensitive LuCaP35 prostate cancer xenografts (ASPC) is attenuated following castration and increases at the time of castration-resistant tumor re-growth (CRPC).

Lucas, et al

SUPPLEMENTARY FIGURE S2

A

	Tmprss2$^{+/+}$; TRAMP	Tmprss2$^{-/-}$;TRAMP
Ki67	66.7%±13.2	72.3%±11.8 p=0.15
Caspase III	4.0% ± 1.6	9.2% ± 5.9 p=0.03

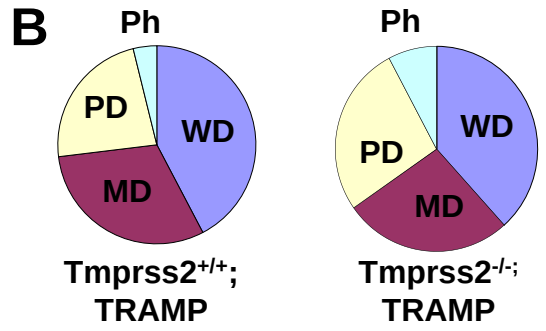

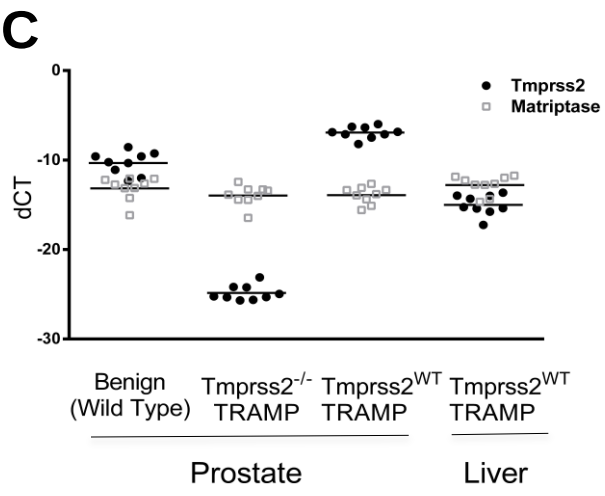

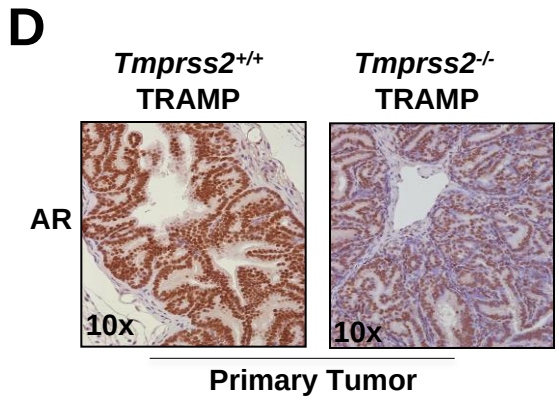

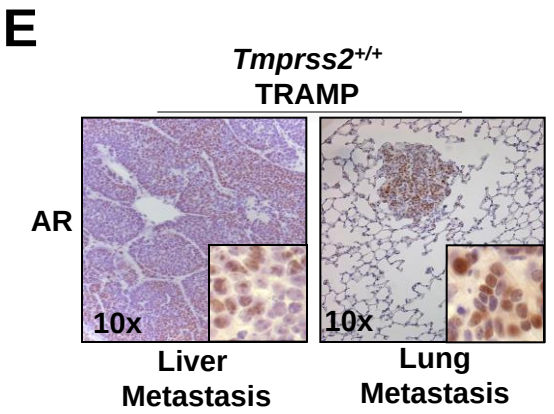

Supplementary Figure S2. Characterization of the differentiation status, Tmprss2 and AR expression in Tmprss2$^{+/+}$ TRAMP and Tmprss2$^{-/-}$ TRAMP mice.

(A) Proliferation and apoptosis rates in Tmprss2+/+;TRAMP (n=16) and Tmprss2-/-;TRAMP (n=17) tumors determined by Ki67 staining and Caspase III staining, respectively.

(B) Tmprss2 genotype and the histological differentiation status of prostate tumors in TRAMP mice. WD: well differentiated, MD: moderately differentiated, PD: poorly differentiated and PH: phylodies like. Poorly differentiated was also characterized by positive staining for the neuroendocrine marker synaptophysin.

(C) Tmprss2 and Matriptase expression determined by qRT-PCR in benign and neoplastic epithelium in the prostate gland and in metastatic tumor foci resected from liver.

(D) Representative example of immunohistochemical assessment of androgen receptor (AR) protein in the prostate glands of Tmprss2+/+;TRAMP and Tmprss2-/-;TRAMP mice. No significant differences in AR staining was observed between genotypes.

(E) Representative example of immunohistochemical assessment of androgen receptor (AR) protein in the liver and lung metastasis from Tmprss2+/+;TRAMP mice. Tumor cells with and without nuclear AR expression (brown immunoreactivity) were evident.

Lucas, et al

SUPPLEMENTARY FIGURE S3

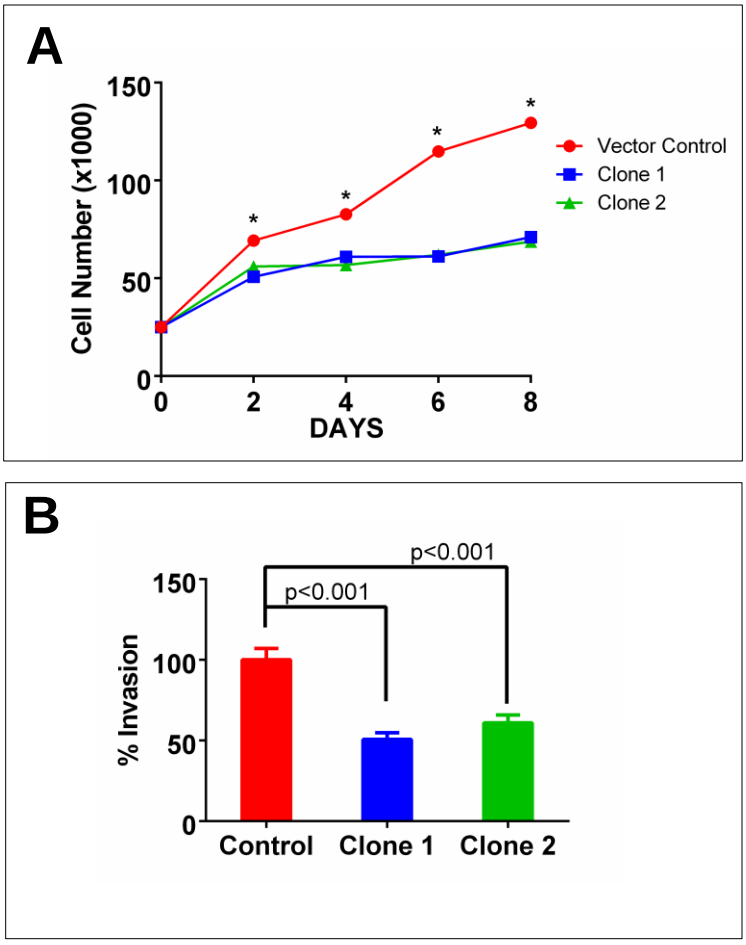

Supplementary Figure S3. Suppression of TMPRSS2 inhibits cell proliferation and invasion.

(A) Suppression of TMPRSS2 reduces the proliferation of LNCaP C4-2B cells. Two distinct shRNAs targeting the TMPRSS2 transcript and control scrambled shRNAs were introduced into LNCaP C4-2B cells. 20,000 cells were plated and The number of metabolically active cells was measured at 0, 2, 4, 6 and 8 days using the Celltiter 96 Cell Proliferation Assay from Promega (Madison, WI). *P<0.05 for differences.

(B) Suppression of TMPRSS2 reduces the invasion of LNCaP C4-2B cells. Differences were determined by Student's T-test.

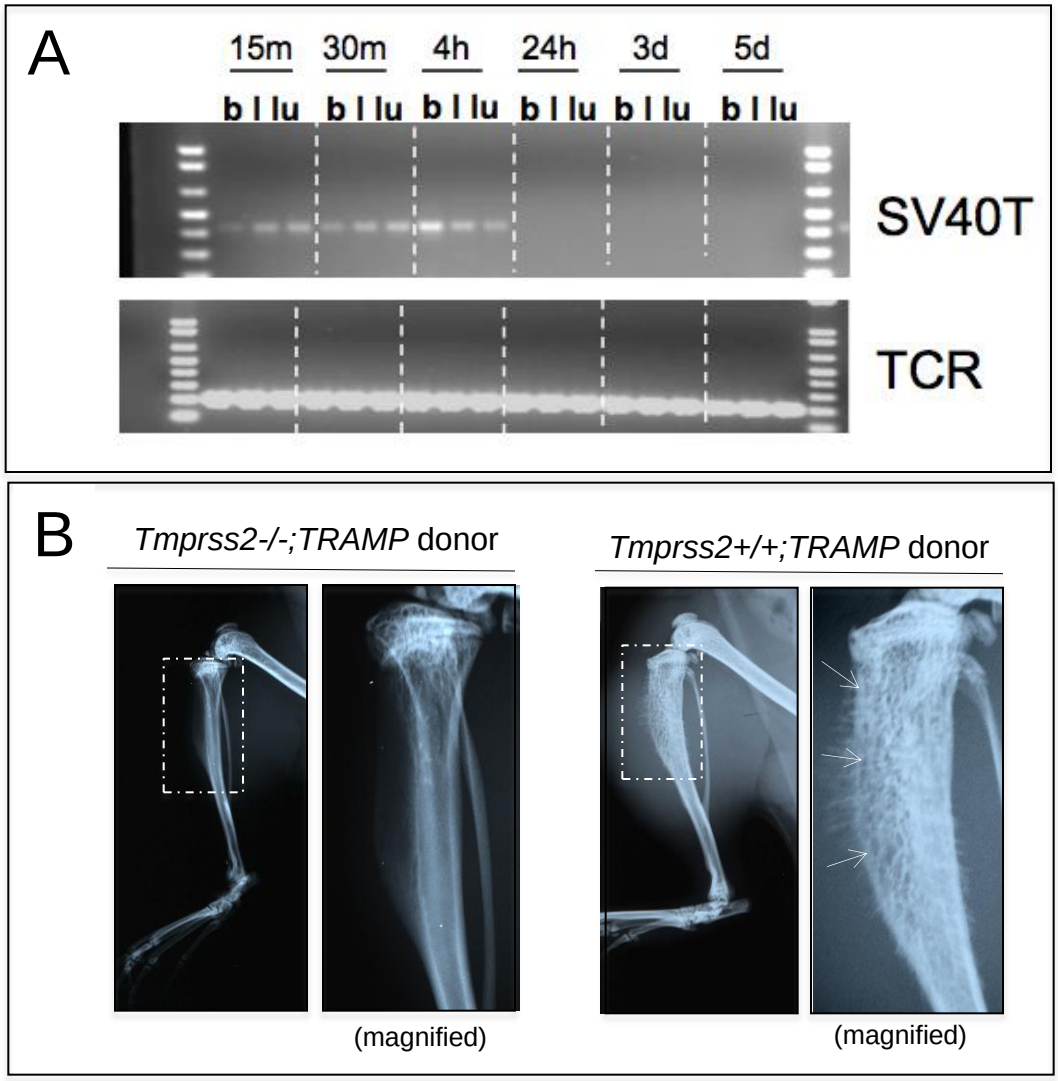

Supplementary Figure S4. **TMPRSS2 influences tumor cell clearance and growth in metastatic sites. (A)** Rapid clearance of non-viable tumor cells following intravenous injection. Tumor cells were dissociated from primary tumors arising in 32 week old Tmprss2+/+;TRAMP mice, fixed in ethanol, washed, resuspended in PBS, and 5 x 10^5 cells were injected into the tail veins of recipient mice. At the indicated time points, mice were euthanized and DNA was extracted for blood (b), liver (l) and lung (Lu) followed by RT-PCR for SV40T antigen or T cell receptor (TCR) as a positive control. **(B)** Cells derived from *Tmprss2*$^{-/-}$;TRAMP or *Tmprss2*^{WT};TRAMP primary tumors were injected directly into the tibia of recipient hosts. Donor tumors were obtained at 20 or 32-week time points. Recipients were imaged and sacrificed at 8 weeks after intratibial injections and tumor presence was confirmed by histology. Representative radiographs of the xenografted mouse tibia are shown. Arrows denote an expansile bone lesion with mixed osteolytic/osteoblastic characteristics. Histological examination determined that 21 of 32 (66%) recipients of tumor cells derived from 6 different *Tmprss2*^{WT};TRAMP donors had tumors, while 0 of 29 recipients of tumors cells from 8 different *Tmprss2*$^{-/-}$;TRAMP donors had evidence of tumor growth ($p<0.001$)

Lucas, et al

SUPPLEMENTARY FIGURE S5

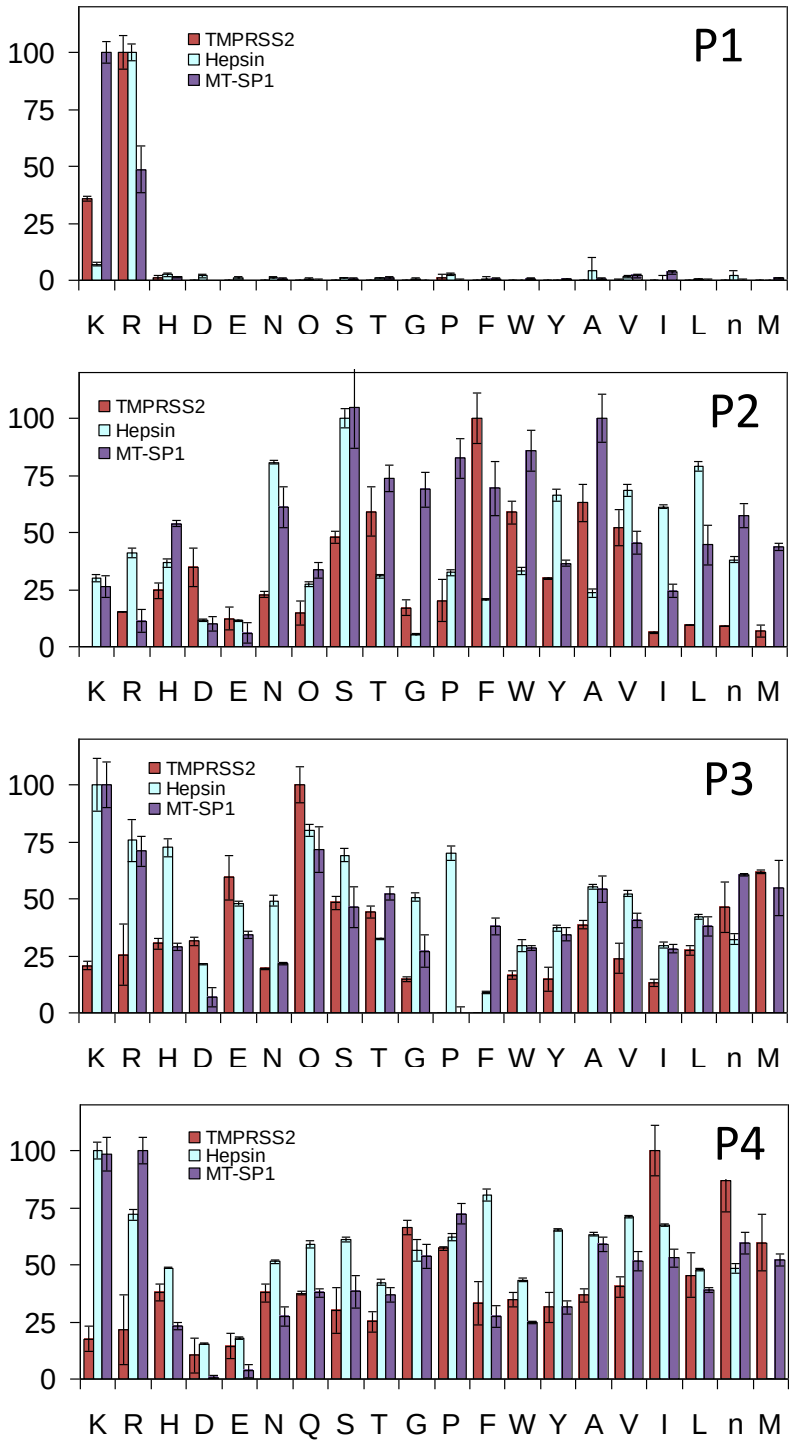

Supplementary Figure S5. Comparison of cleavage specificities for type II transmembrane serine proteases expressed in prostate epithelium. Comparative PS-SCL analysis of the extended substrate specificities of TMPRSS2 (Red), Hepsin (blue), and Matriptase (purple) demonstrates diversity in the preferred P2-P4 cleavage site residues.

Supplementary Figure S6. Identification of putative TMPRSS2 substrates based on peptide cleavage specificities determined by PS-SCL.

P4	P3	P2	P1	P'	Gene	Name	Source	Accession	Predicted
A									
G	E	T	R	IIKG	KLK11	Kallikrein-related peptidase 11	UniProt	Q9UXB7	GETR
P	Q	A	R	ITGG	PRSS8	prostasin [S01.159]	UniProt	Q16651	PQAR
P	Q	F	R	IKGG	PLAT	t-plasminogen activator [S01.232]	UniProt	P00750	PQFR
B									
P	Q	G	R	IVGG	F7	coagulation factor VIIa [S01.215]	UniProt	P08709	PQGR
P	S	A	R	IVGG		polyserase-2 unit 1 [S01.414]	ProtID	CAF25303	PSAR
S	M	T	R	VVGG	F12	coagulation factor XIIa [S01.211]	UniProt	P00748	SMTR
R	Q	A	R	VVGG	ST14	matriptase [S01.302]	UniProt	Q9Y5Y6	RQAR
G	G	V	R	IVGG	ACR	acrosin [S01.223]	UniProt	P10323	GGVR
L	M	A	R	IFNG	MASP1	mannan-binding lectin-associated serine peptidase 1 [S01.198]	UniProt	P48740	LMAR
I	Q	S	R	IVGG	KLK2	kallikrein-related peptidase 2 [S01.161]	UniProt	P20151	IQSR
I	Q	S	R	IVGG	KLK1	kallikrein 1 [S01.160]	UniProt	P06870	IQSR
C									
I	K	P	R	IVGG	F11	coagulation factor XIa [S01.213]	UniProt	P03951	IKPR
N	L	T	R	IVGG	F10	coagulation factor Xa [S01.216]	UniProt	P00742	NLTR
D	F	T	R	VVGG	F9	coagulation factor IXa [S01.214]	UniProt	P00740	DFTR
I	F	S	R	ILGG		ovochymase-2 [S01.320]	ProtID	XP_089945	IFSR
S	G	T	R	IAEG		secreted trypsin-like serine peptidase homologue [S01.957]	MEROPS	NA	SGTR
P	R	G	R	ILGG	CFD	complement factor D [S01.191]	UniProt	P00746	PRGR
R	Q	K	R	IIGG	PRSS12	neurotrypsin [S01.237]	UniProt	P56730	RQKR
I	D	G	R	IVEG	F2	thrombin [S01.217]	UniProt	P00734	IDGR
R	Q	S	R	IVGG	TMPRSS2	epitheliasin [S01.247]	UniProt	O15393	RQSR
S	E	Q	R	ILGG	TMPRSS11D	adrenal secretory serine peptidase [S01.047]	UniProt	O60235	SEQR
T	N	A	R	VVGG	ELA1	elastase-1 [S01.153]	UniProt	Q9UNI1	TNAR
A	L	T	R	IVGG	TMPRSS9	polyserase-1A unit 3 [S01.969]	UniProt	Q7Z410	ALTR
P	S	S	R	IVGG	TMPRSS6	matriptase-2 [S01.308]	UniProt	Q8IU80	PSSR
I	L	S	R	IVGG	KLK3	kallikrein-related peptidase 3 [S01.162]	UniProt	P07288	ILSR
M	S	S	R	IVGG	PRSS33	tryptase-6 [S01.075]	UniProt	Q8NF86	MSSR
K	P	T	R	VVGG	TMPRSS9	polyserase-IA unit 2 [S01.358]	UniProt	Q7Z410	KPTR
P	V	D	R	IVGG	HPN	hepsin [S01.224]	UniProt	P05981	PVDR
P	S	S	R	VVNG	ELA3B	pancreatic endopeptidase E form B [S01.205]	UniProt	P08861	PSSR
M	A	G	R	IVGG	TMPRSS9	polyserase-IA unit 1 [S01.357]	UniProt	Q7Z410	MAGR
M	N	K	R	ILGG	CORIN	corin [S01.019]	UniProt	Q9Y5Q5	MNKR
L	S	A	R	VVGG	CTRC	chymotrypsin C [S01.157]	UniProt	Q99895	LSAR
G	L	S	R	IVNG	CTRB2	chymotrypsin B [S01.152]	UniProt	Q6GPI1	GLSR
P	V	Q	R	ILGG	HP	haptoglobin-1 [S01.972]	UniProt	P00738	PVQR
I	T	S	R	IVGG	PRSS21	testisin [S01.011]	UniProt	Q9Y6M0	ITSR
T	S	T	R	IVGG	KLKB1	plasma kallikrein [S01.212]	UniProt	P03952	TSTR
M	T	G	R	IVGG	TMPRSS13	TMPRSS13 peptidase [S01.087]	UniProt	Q9BYE2	MTGR
Y	V	T	R	VVGG	ELA2A	pancreatic elastase II [S01.155]	UniProt	P08217	YVTR

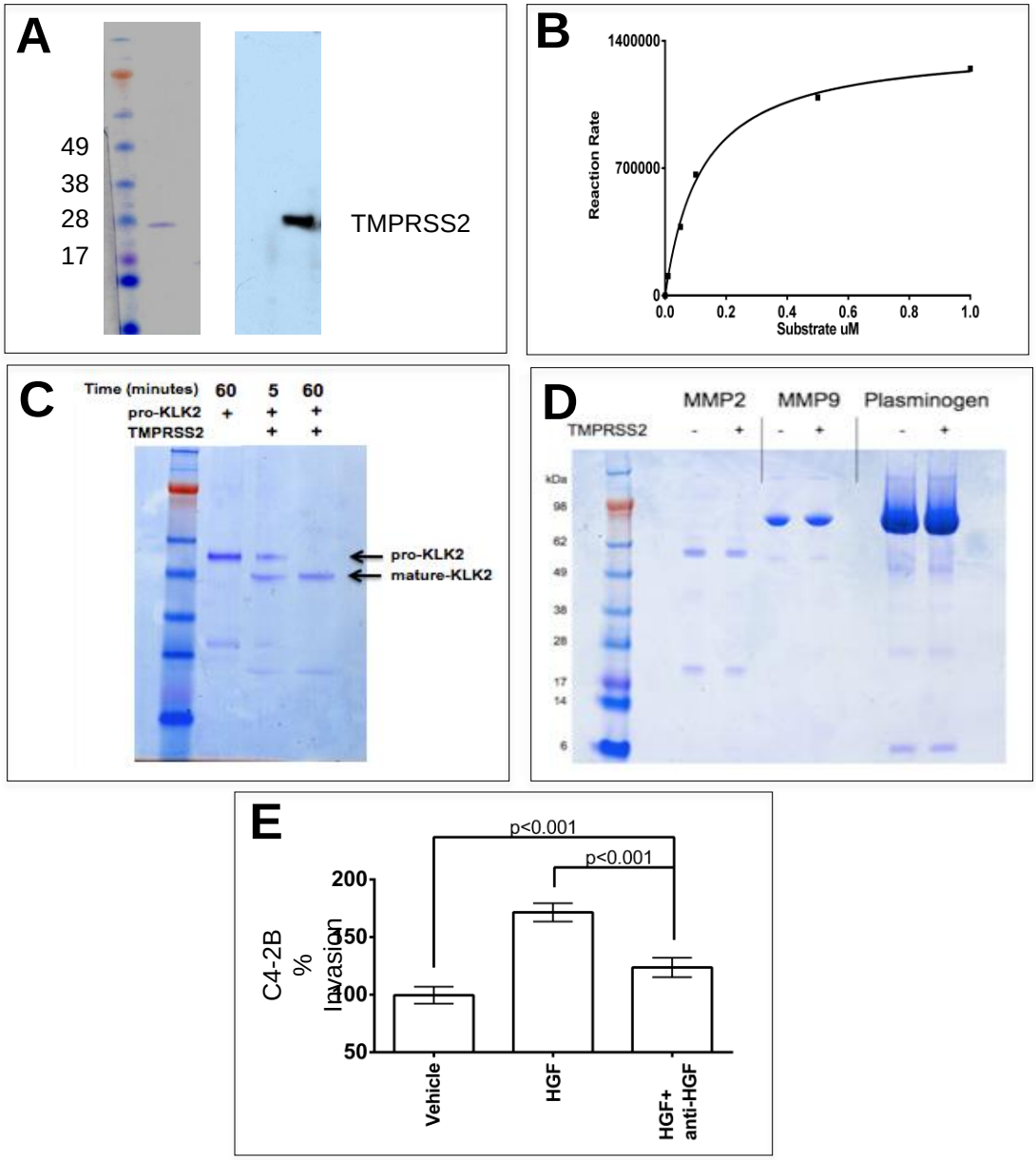

Supplementary Figure S7. Assessment of TMPRSS2 substrate activity.
(A) Coomassie blue stained SDS-page gel of recombinant human TMPRSS2 expressed in *Pichia pastoris*. Immunoblot using a monoclonal antibody raised against the protease domain of TMPRSS2.
(B) TMPRSS2 activity against multiple concentrations of the fluorogenic substrate Boc-GLN-ALA-ARG-Mec. Apparent Km=0.1191 μM. Inhibition of TMPRSS2 by identified compounds. Data shown is the mean of three independent assays. The IC50 was determined using nonlinear regression analysis.
(C) The prostate serine protease KLK2 is a TMPRSS2 substrate. Recombinant active TMPRSS2 is able to proteolyze pro-KLK2 to mature active KLK2. Lane 1: pro-KLK2-GST. Lane 2: pro-KLK2-GST + TMPRSS2, 5 minutes. Lane 3: pro-KLK2-GST + TMPRSS2, 60 minutes.
(D) TMPRSS2 does not proteolyze MMP2, MMP9 or Plasminogen. Each substrate was incubated with TMPRSS2 for 60 minutes.
(E) Exposure of C4-2B cells natively expressing TMPRSS2 to HGF increases invasion compared to vehicle treated cells (p<0.001). The pro-invasive effect is abolished with concurrent treatment with HGF neutralizing antibody (p<0.001).

Lucas, et al

SUPPLEMENTAL FIGURE S8

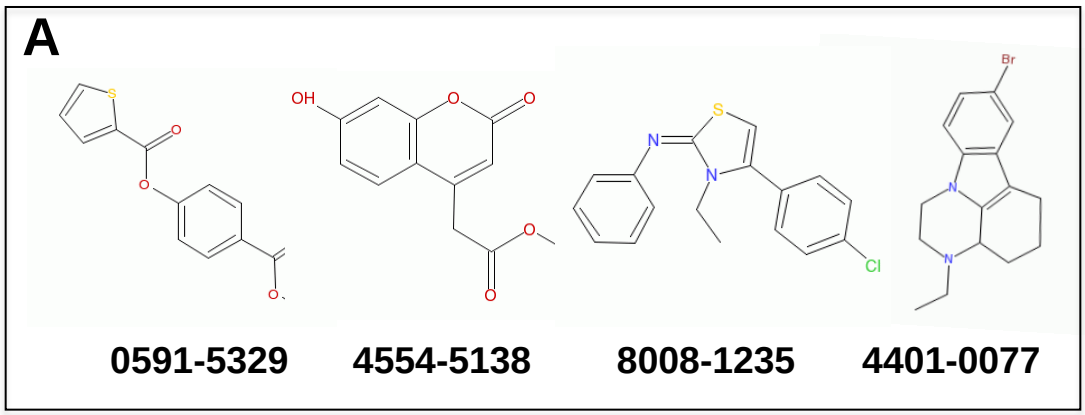

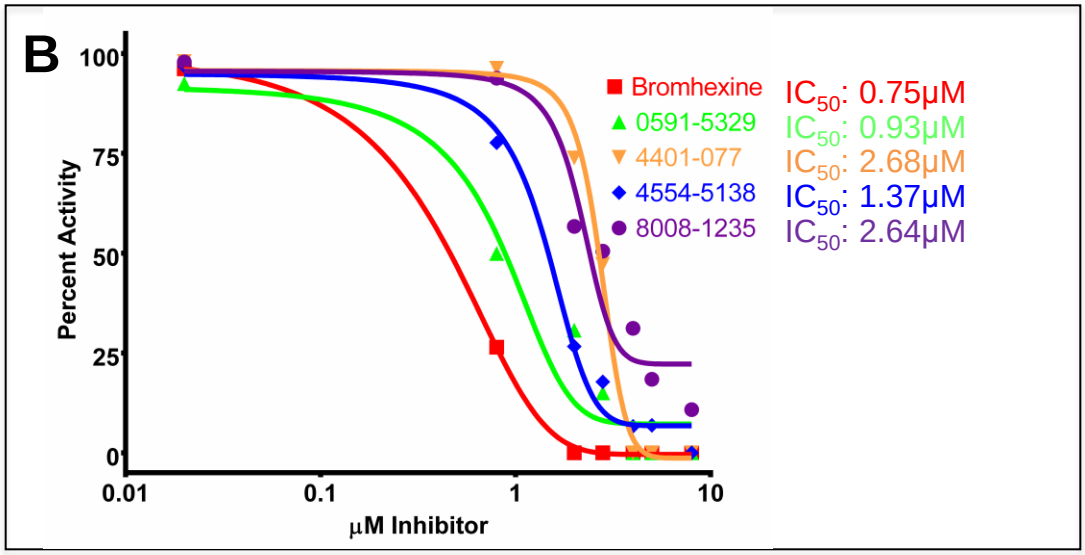

C

	TMPRSS2	Hepsin	Matriptase	Trypsin	Thrombin
Bromohexine	0.75	35.34	58.97	>100	>100
0591-5329	0.93	54.98	75.34	98.35	>100
4401-077	2.68	>100	>100	>100	>100
4554-5138	1.37	87.23	78.27	95.12	>100
8008-1235	2.64	>100	>100	>100	>100

Supplementary Figure S8. Characterization of TMPRSS2 chemical inhibitors.

(A) Chemical structures of the TMPRSS2 inhibitors identified by screening compound libraries. **(B)** Inhibition of TMPRSS2 activity by the identified compounds. Purified recombinant TMPRSS2 was preincubated with indicated compounds for 30 min at room temperature. The residual percent activity of the enzyme toward the chromogenic substrate was then determined using a kinetic microplate reader at 405 nm. Data are the mean of three independent experiments. IC50 was calculated by four-variable nonlinear regression curve fitting.
(C) IC50 values in uM for each compound identified in the TMPRSS2 inhibitor screen toward 5 serine proteases.

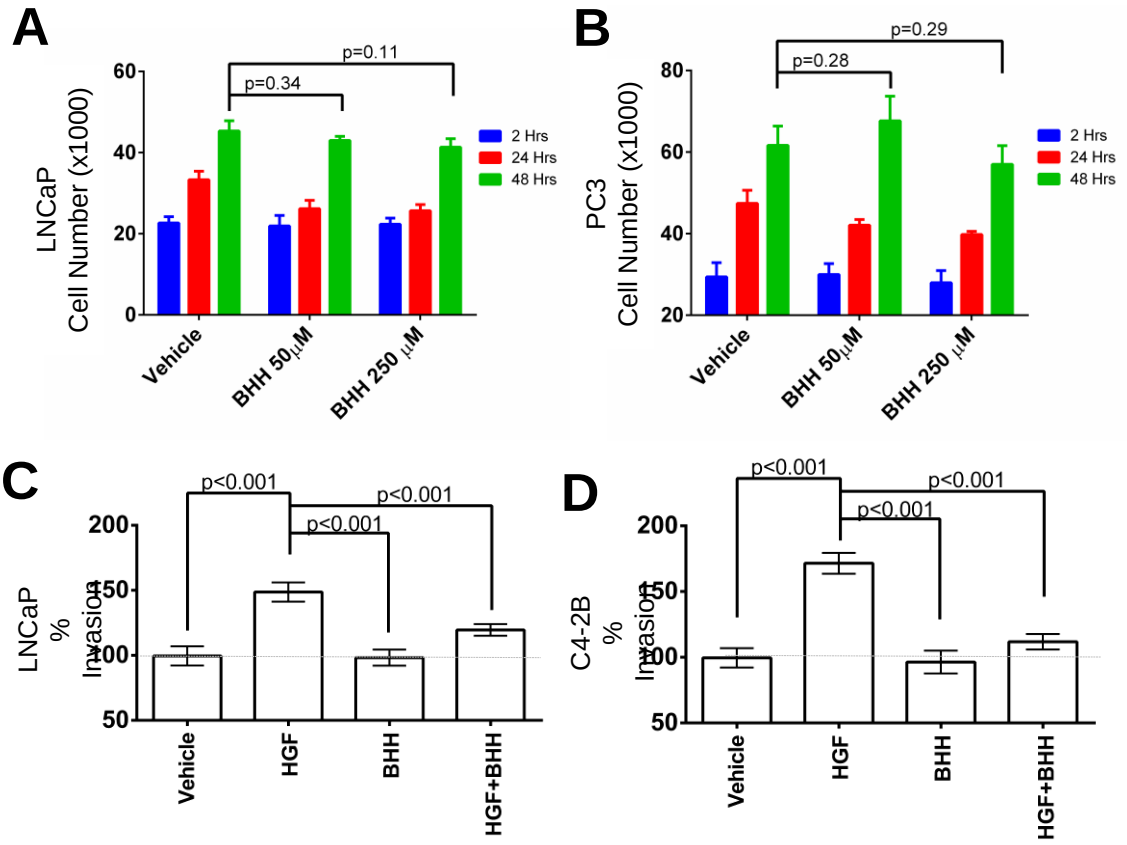

Supplementary Figure S9. Bromhexine suppresses prostate cancer cell invasion but but does not influence proliferation *in vitro*.

Effects of bromhexine (BHH) on LNCaP **(A)** and PC3 **(B)** cell viability. Cell lines were plated at a density of 2000 cells/well in a 96-well tissue culture plate in replicates of 8. Cells were treated with vehicle or the indicated concentration of BHH. The number of metabolically active cells was measured at 2, 24, and 48 hours using the Celltiter 96 Cell Proliferation Assay from Promega (Madison, WI).

Effects of bromhexine (BHH) on LNCaP **(C)** and C4-2B **(D)** invasion. 50,000 cells were plated with serum free media into the upper matrigel coated invasion chamber and allowed to invade for 24 hours toward the lower chamber which contained serum-free media with vehicle, 50 ng of sc-HGF, and/or 250 μM BHH. Invaded cells were detached, lysed, stained and counted in a fluorescence plate reader.